International Symposium of Research Students on Materials Science and Engineering
December 20-22, 2004, Chennai, India
Department of Metallurgical and Materials Engineering, Indian Institute of Technology, Madras

SYNTHESIS, STRUCTURE AND ELECTRICAL CONDUCTION BEHAVIOUR OF THE SYSTEM $Sr_{1-X}Nd_XTi_{1-X}Mn_XO_3$ ($x \leq 0.50$)

Prakash Singh, C.R. Gautam, Sindhu Singh, Devendra Kumar and Om Parkash
Department of Ceramic Engineering, Institute of technology,
Banaras Hindu University, Varanasi-221005

ABSTRACT

Attempts were made to synthesize various compositions in the system $Sr_{1-x}Nd_xTi_{1-x}Mn_xO_3$ ($x \leq 0.50$) by solid-state ceramic route. XRD patterns confirmed single-phase formation in all the compositions investigated. Crystal structure remains cubic similar to $SrTiO_3$ for the compositions with x=0.20 and becomes orthorhombic for reaming compositions similar to $NdMnO_3$. Lattice parameter increasing with increasing x up to 0.10. Density and porosity have been determined. It was found that bulk density for various samples were greater than 90% of theoretical value. Seebeck coefficient was measured on thick pellet in the temperature range 300K – 1000K. Initially Seebeck coefficient was found to be positive indicating that holes are majority charge carriers near room temperature. α, changes from positive to negative with increasing temperature indicating electrons become majority charge carrier at elevated temperatures near 1000 K for all the compositions. DC and AC conductivity were measured in the temperature range 300K-1000K and 300K-500K respectively. It is observed that conductivity increases with increasing x. On the basis of variation of α, DC conductivity and AC conductivity with temperature an understanding of the electrical conduction behaviour of this system is developed.

Keywords: Perovskite oxides, strontium titanate, electrical conduction.

1. INTRODUCTION

Strontium titanate doped with donor ions such as rare earth or bismuth on the strontium sites exhibits relaxor behaviour. During the last 15 years, valence compensated solid solutions based on $SrTiO_3$ have been studied extensively[1-4]. These have the general formula $Sr_{1-X}La_XTi_{1-X}M_XO_3$ (where M= Fe, Co and Ni etc.). It has been reported that solid solution forms over a wide range of compositions in many systems. Polycrystalline samples of Mn and/ or La doped $SrTiO_3$ are interesting for their electrical properties[5-8] , strictly dependent on the grain boundaries where the perovskite structure may be affected by oxygen vacancies and the doping concentration may be high and inhomogeneous. Different manganese environments were evidenced with different concentrations both in Mn^{4+} and Mn^{2+} oxidation states, and two perovskite type phases were observed, one of them increasing with Mn addition and related to heavy doped disordered regions. Only weak and narrow EPR signals, from a small fraction of Mn^{2+} and Mn^{4+} ions were observed when the La and Mn content did not exceed 5%, indicating the nearly complete stablisation of the Mn^{3+}, however for heavily substitutes samples, a complex dynamics of Mn^{3+} stablisation is suggested[9] . In view of interesting properties exhibited by the above systems it is worthwhile to investigate the analogous system $Sr_{1-x}Nd_xTi_{1-x}Mn_xO_3$. In this paper we report the preparation and characterization of the electrical conduction behaviour of this system prepared by the solid state ceramic method.

2. EXPERIMENTAL PROCEDURE

Various compositions of the system $Sr_{1-x}Nd_xTi_{1-x}Mn_xO_3$ ($x \leq 0.50$) were prepared by the solid-state method. The raw materials $SrCO_3$, Nd_2O_3, TiO_2 and $MnCO_3$ all having purity above to 99 % were used. Appropriate quantities of these materials were weighed accurately and ball milled in an agate jar using acetone as a liquid media. The dried powders were calcined at 1473 K for 12 h and then furnace cooled. The resulting powders were ground and mixed with 2% PVA and pressed as cylindrical pellets (dia.12 mm) with an optimum load of 70 KN. The pellets were slowly heated up to 873 K and then held at this temperature for 1 h to burn off the binder. Thereafter the temperature was raised to 1573 K, the pellets were sintered at this temperature for 12 h. The sintered pellets were reground, palletized and sintered at 1573 further for 12 h.

XRD patterns were recorded by X-ray Rigaku Diffractometer on powder samples. Seebeck coefficient was measured as a function temperature (300K-1000K) on thick pellet of thickness ~ 7mm. and Escort EDM 3150 Multimeter used to record voltage. For the measurement of DC Resistivity and AC conductivity sintered pellets were polished using emery paper 0/0, 1/0, 2/0,3/0, 4/0 and 5/0, Ag-Pd paint was used for electroding the samples. DC resistivity measurements have been made in the temperature range 300K-1000K using Keithley 617 Programmable Electrometer. AC Conductivity were measured as a function of temperature (300K-500K) in the frequency range of 100Hz-2MHz using Hioki 3532 HiTester LCR Meter.

3. RESULTS AND DISCUSSIONS

Formation of single phase was confirmed by the absence of characteristic XRD lines of the constituent oxides. Powder XRD data of the compositions with x up to 0.10 were indexed on the basis of cubic unit cell similar to $SrTiO_3$[1] and other compositions were index on the basis of orthorhombic unit cell similar to $NdMnO_3$. The lattice parameter 'a' for various composition is given in Table 1. Experimental density increases with increasing concentration of dopant i.e. Nd and Mn indicate that sinterbility increases at same firing temperature.

Plots of log of DC resistivity, ρ_{dc} with inverse of temperature, 1000/T for all the compositions with x = 0.01, 0.05, 0.10, 0.20, 0.30 and 0.50 are shown in Fig. 1. Initially these plots indicate that there is slight increase in resistivity with temperature for the composition with x=0.01, 0.05 and 0.10. Temperature at which resistivity starts to decrease shift towards lower temperature as dopant concentration increases. For compositions with x=0.20 to 0.50 at high temperature resistivity almost becomes independent of temperature. These plots are found to have two linear regions for composition with x up to 0.10 and one linear region for all other compositions obeying Arrhenius relationship

$$\rho_{dc} = \rho_0 \exp(E_a/kT) \qquad \text{…….(1)}$$

where E_a is the activation energy for conduction and k is the Boltzmann constant.
The values of activation energies obtained by least square fitting of the resistivity data for various compositions are given in Table2. It is also observed that conductivity increases with increasing x. Initially the increase in resistivity value for x =0.01, 0.05 and 0.10 may be due to the following processes:

$$Nd_2O_3 + 2TiO_2 \xrightarrow{Sr\,TiO3} 2Nd_{Sr}^{\bullet} + 2Ti_{Ti} + 6O_o + 2e^{/} + 1/2O_2 \qquad (2)$$

$$2SrO + Mn_2O_3 + 1/2O_2 \xrightarrow{SrTiO3} 2Sr_{Sr} + 2Mn_{Ti}^{/} + 6O_o + 2h^{o} \qquad (3)$$

$$2SrO + 2MnO + 1/2O_2 \xrightarrow{SrTiO3} 2Sr_{Sr} + 2Mn_{Ti}^{//} + 5O_o + 2h^{o} \qquad (4)$$

$$O_o \longrightarrow 1/2\,O_2 + V_O^{\bullet\bullet} + 2\,e^{/} \qquad (5)$$

Here complete compensation of charge carriers created in above reaction (2) and (3) takes place. Hence resistivity increases initially. The observed p-type conductivity is due to presence of Mn in +2 state. This produces hole as per equation (4). As doping increases, the concentration of Mn^{2+} and Mn^{3+} increases and hopping conduction between these localized states dominates.

Plots of α Vs T for compositions with x = 0.01, 0.05, 0.10 and 0.30 are shown in Fig. 2. It is observed that for the composition with x=0.01 and 0.05, α remains constant up to a particular temperature beyond which there is sudden decrease and becomes negative at higher temperature where as for composition with x=0.10 and 0.30 there is gradually decrease in value of α on increasing temperature. The temperature at which α changes sign from positive to negative shift towards the lower temperature side as dopant concentration increases. α is found to be positive for all the compositions at room temperature indicating that holes are the majority charge carriers. At high temperature α changes form positive to negative sign indicating that electrons are the majority charge carries.

This may be due to fact that the major defects present in these materials are oxygen ion vacancies. These vacancies exist as doubly positively charged, $V^{\bullet\bullet}_o$ above 1000 K and as singly ionized, $V^{\bullet}_o$ at room temperature[10]. Singly positively charged $V^{\bullet}_o$ will ionize as:

$$V^{\bullet}_o \Leftrightarrow V^{\bullet\bullet}_o + e^{/} \qquad (\text{at} \sim 825\ \text{K}) \qquad \text{…….(6)}$$

This reaction produces electrons in the conduction band. The sudden decrease observed in the value of α around 800 K (except for composition with x=0.30) and change in its sign in these materials may be due to above process. The conductivity above this temperature will have additional activation energy due to above reaction, which is reported to be in the range 0.70-0.80 eV[11]. This explains the observed change in activation energy (Table 2) in the two temperature regions or the change in slope of log ρ_{dc} vs 1000/T plots at ~ 850 K

Plots of logσ_{ac} vs.1000/T at 10 KHz for x= 0.01, 0.05, 0.20, 0.30 and 0.50 are shown in Fig.3. From these plots it is observed that, initially on increasing temperature, there is decrease in ac conductivity up to a particular temperature beyond which conductivity increases with increasing temperature for the compositions with x up to 0.10. AC conductivity increases with increasing temperature for all other compositions with increasing temperature. In the high temperature region the linear variation of logσ_{ac} with inverse of temperature suggest the validity of the equation:

$$\sigma = \sigma_0 \exp(-E_a/kT) \qquad \text{…….(7)}$$

where E_a is the activation energy for AC conductivity. Table 2 gives the activation energy values at different temperatures for the various compositions.

Plots of log σ_{ac} vs. logf for all the compositions at temperature 400K are shown in the Fig. 4. Behaviour of log σ_{ac} vs. logf plots for various samples is essentially similar .A plateau is observed in the low frequency region followed by a frequency dispersion region. This plateau shifts towards the higher frequency side as temperature increases. It is also observed that at a particular temperature this plateau moves on higher frequency side as doping concentration increases. The DC conductivity, σ_{dc} ($\omega \rightarrow 0$) can be obtained by extrapolating the low frequency plateau to $\omega \rightarrow 0$ at a few temperatures. Fig. 6 shows the variation of log σ_{dc} with inverse of

temperature for the compositions with x=0.05, 0.10, 0.20, 0.30 and 0.50. All these plots are linear showing that conductivity follows Arrhenius relationship

$$\sigma_{DC} = \sigma_0 \exp [-E_a/kT] \quad \text{……. (8)}$$

where E_a is the activation energy for conduction and k is Boltzmann's constant. Ea for composition with x=0.05 and x= 0.30 is 0.32 eV, and for composition with x= 0.10 and 0.20 it is 0.38, where as for composition with x = 0.50 it is 0.20 eV.

In polycrystalline ceramic materials, the defects structure and hence the electrical conduction are different for grain and grainboundaries. Plots of log σ_{ac} vs log f of these materials show frequency independent regions (plateaus) connected by frequency dependent regions. Generally one should get a plateau at low frequencies which represents the total conductivity of the sample followed by frequency dependent region in which, the relaxation of grain boundaries processes occur. This is followed by another plateau in the high frequency region, which represents the contribution of the grains (bulk) to the total conductivity. A frequency region occurs after the high frequency plateau, representing relaxation of bulk process. One can get the contributions of grainboundaries to the total conductivity from the difference of the conductivity values corresponding to high and low frequency plateaus. Due to limitation of our measuring instrument we could not observe these regions as discussed above.

4. CONCLUSION

Single phase forms for all compositions investigated. Structure remains cubic like $SrTiO_3$ for the compositions with x up to 0.20 and orthorhombic like $NdMnO_3$ for remaining compositions. Initially Seebeck coefficient is positive indicating that holes are majority charge carriers and at high temperature it changes to negative sign indicating that electrons are majority charge carriers for all the compositions. Conductivity increases with increasing dopant concentration (i.e. Nd & Mn).

ACKNOWLEDGEMENT

Financial support from Defence Research and Development Organization (DRDO), India is gratefully acknowledged.

REFRENCES

1. Prasad Ch D, Kumar D, and Parkash Om, *Phys. Stat. Sol. (a)* 116 (1989) p K81.
2. Upadhyay S, Kumar D, and Parkash Om, *Trans. Ind. Cer. Soc.* 56 (1997) p 96.
3. Dwivedi R K, Kumar D, and Parkash Om, *J. Phys. D. Appl. Phys.*33 (2000) p 88.
4. Dwivedi R K, Kumar D, and Parkash Om, *Brit. Cer. Trans.* 100 (2001) p 115.
5. Ravikumar V, Rodregues RP, and Dravid VP, *J. Phys. D: Appl. Phys.* 29 (7) (1 996) p 1799.
6 Rodrigues RP, Chand H, Ellis DE, and Dravid VP, *J. Am. Ceram. Soc.* 82(9) (1999) p 2373.
7. Rodrigues RP, Chand H, Ellis DE, and Dravid VP, *J. Am. Ceram. Soc.* 82(9) (1999) p 2385.
8 Rodrigues RP, Chand H, Ellis DE, and Dravid VP, *J. Am. Ceram. Soc.* 82(9) (1999) p 2395.
9 C B Azzoni, M C Mozzati, P Galinetto, A Paleari, V Massarotti, M Binni, and D. Capsoni, *Solid State Comms.* 116, (2000) p 303

10. Moss R, and Hardtle KH, *J. Appl. Phys.* 80 (1996) p 393.
11. Long SA and Blumenthal RN, *J. Am. Ceram. Soc.* 54 (1971) p 577.

TABLES

Table 1. Composition, Lattice parameter, structure, experimental density of different compositions in the system $Sr_{1-x}Nd_xTi_{1-x}Mn_xO_3$.

Composition	Lattice Parameter (A^0)			Structure	Experimental Density (gm/cm^3)
	a	b	c		
X = 0.01	3.8860	-	-	Cubic	4.719
X = 0.05	3.8865	-	-	Cubic	4.863
X = 0.10	3.9112	-	-	Cubic	4.885
X = 0.20	3.8844	-	-	Cubic	5.015
X = 0.30	5.4699	5.8898	7.3987	Orthorhombic	5.337
X=0.50	5.4120	5.7696	7.4921	Orthorhombic	5.463

Table.2: The activation energy for DC conduction and AC conduction at 10 KHz for different compositions in the system $Sr_{1-x}Nd_xTi_{1-x}Mn_xO_3$.

Composition	Temperature Range (K)	Activation Energy (DC) (ev)	Temperature Range (K)	Activation Energy (AC) (ev)
X = 0.01	390-600 600-1000	0.50±.01 1.32±0.01	440-500	0.16±0.01
X = 0.05	330-630 630-1000	0.42±0.01 0.74±0.01	335-500	0.20±0.03
X = 0.10	330-750 750-1000	0.41±0.01 0.67±0.01	335-500	0.29±0.01
X = 0.20	330-750	0.40±0.03	365-500	0.40±0.02
X = 0.30	300-750	0.36±0.03	425-500	0.45±0.02
X = 0.50	350-750	0.15±.02	300-500	0.19±0.01

FIGURES

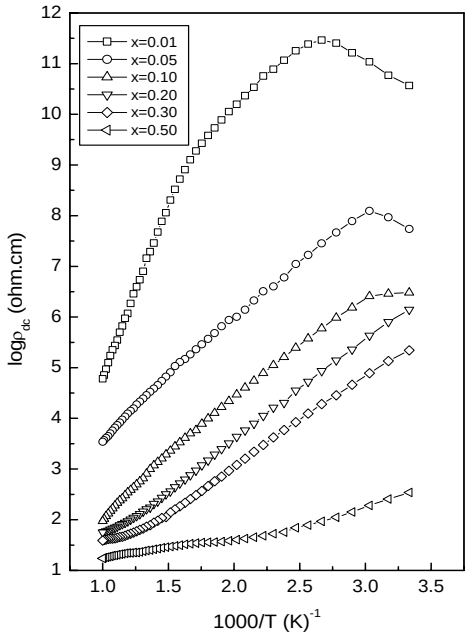

Fig.1Variation of log of DC resistivity, logρ_{dc} with inverse of temperature for different compositions in the system $Sr_{1-x}Nd_xTi_{1-x}Mn_xO_3$.

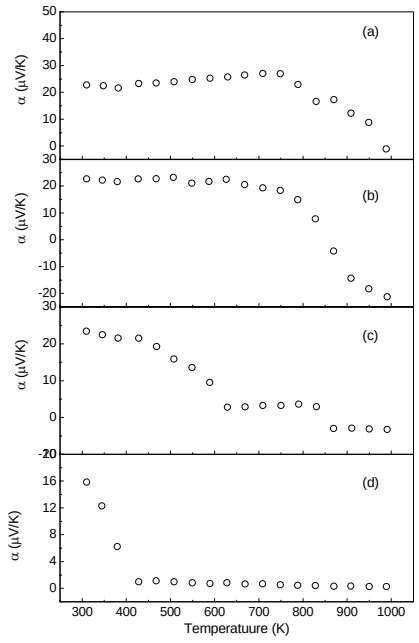

Fig.2 Variation of Seebeck Co-efficient, with temperature for composition with x (a) 0.01 (b) 0.05 (c) 0.10 and (d) 0.30 in the system $Sr_{1-x}Nd_xTi_{1-x}Mn_xO_3$

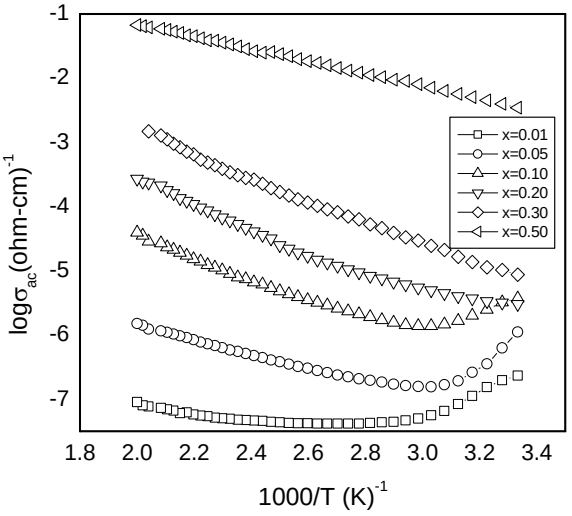

Fig.3 Variation of log of AC conductivity, $\log\sigma_{ac}$ with inverse of temperature for different compositions in the system $Sr_{1-x}Nd_xTi_{1-x}Mn_xO_3$ at 10 KHz

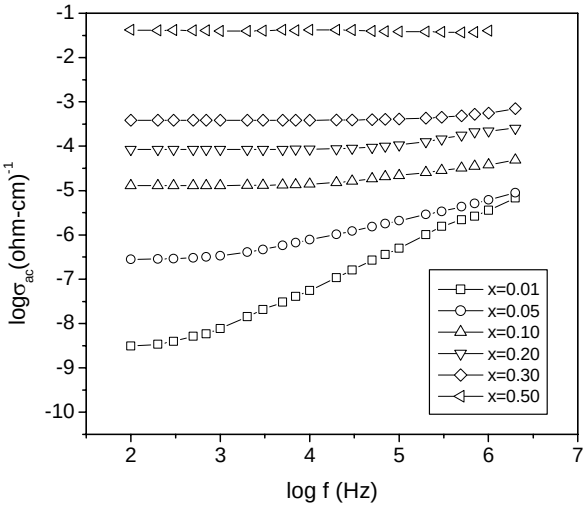

Fig.4 Variation of log of AC conductivity, $\log\sigma_{ac}$ with log of frequency for different compositions in the system $Sr_{1-x}Nd_xTi_{1-x}Mn_xO_3$ at 400 K.

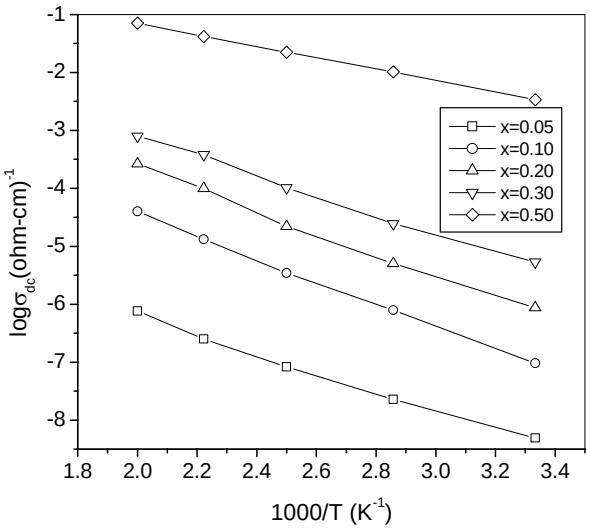

Fig.5 Variation of log σ_{dc} with 1000/T for different compositions in the system $Sr_{1-x}Nd_xTi_{1-x}Mn_xO_3$